

Experimental and numerical investigation of a meandering jet in shallow rectangular reservoirs under different hydraulic conditions

Erica Camnasio¹, Michel Pirotton², Sébastien Erpicum², Benjamin Dewals²

¹ Department of Hydraulic, Environmental, Infrastructures and Surveying Engineering (DIIAR), Politecnico di Milano, Italy

E-mail: erica.camnasio@polimi.it

²Hydraulics in Environmental and Civil Engineering (HECE), University of Liège, Belgium

Email: b.dewals@ulg.ac.be

Abstract

A central meandering jet in shallow rectangular reservoirs has been investigated numerically by the model WOLF2D, on the basis of experimental evidence of this type of flow field in two different setups at different scales. A sensitivity analysis has been conducted with respect to the main parameters of the model. The oscillation frequency of the transversal velocity and the characteristic Strouhal number have been calculated for different Froude numbers. A logarithmic relationship has been found between the Strouhal and the Froude numbers.

1. Introduction

Recent research has underlined the role of the geometrical and hydraulic boundary conditions in the determination of the type of flow pattern which develops in rectangular shallow reservoirs (Dufresne et al., 2010; Camnasio et al., 2011). In the cited papers, different types of flow patterns have been identified and classified as a function of non-dimensional parameters describing the reservoir geometry (e.g., aspect ratio, expansion ratio, ...). The observed flow patterns include plug flows, symmetric and asymmetric patterns with up to two reattachment points on either side-wall of the reservoir. The considered reservoirs are endowed with free-surface inlet and outlet channels placed at the centre of the upstream and downstream reservoir cross-sections.

We present here a new type of flow pattern observed for specific hydraulic conditions and which has not been investigated before. It corresponds to a meandering flow field, characterized by periodical oscillations of the main jet which develops along the axis of the reservoir. It shows some similarities with periodic flows which can be observed in turbulent wakes in shallow flows (e.g., Chen & Jirka, 1995).

The existence of the meandering flow patterns was assessed experimentally in two different experimental rectangular reservoirs, at two different scales. Both setups have a length-to-width ratio $L/B = 1.5$ and an expansion ratio $B/b = 16$, where L is the length of the reservoir, B its width and b the width of the inlet free-surface channel. Notations are defined in Figure 1.

The objective of the present work is threefold:

- define the hydraulic conditions in which the meandering flow pattern develops;
- calculate the period of oscillation of the jet, using numerical simulations based on the academic code WOLF2D,

- determine whether a relationship can be found between the oscillation frequency of the jet and the hydraulic conditions.

In non dimensional terms, the third step consists mainly in investigating a possible link between the Strouhal and the Froude numbers.

2. Previous studies

Literature about meandering water jets in reservoirs is very limited. An example of the study of oscillating flows can be found in the papers of Honeylands and Molloy (1995) and of Davidson and Lawson (1999). The field of application was however very different, since it concerned confined jets in rectangular cavities during the process of steel casting.

The existence of meandering flows in free surface reservoirs was observed qualitatively by Kantoush (2008) in a reservoir characterized by $L = 6$ m, $B = 4$ m and $b = 0.25$ m, and located at Ecole Polytechnique Federale de Lausanne (EPFL). Meandering flow patterns were found for water depths below 0.15 m. Nevertheless, neither the oscillation frequency nor any other quantitative characteristics of the phenomenon were measured.

During these experiments, the discharge was kept constant ($Q = 7$ l/s) while the water depth was varied. Consequently, not only the non-dimensional water depth h/b was changed, but also the inlet Froude number $Fr_{in} = Q/[bh(gh)^{0.5}]$. The inlet Reynolds number was fixed during all experiments: $Re_{in} = 4 Q/(b\nu) = 112,000$, with ν referring to the kinematic viscosity of water.

A similar procedure has been followed for the experiments and simulations presented here. In future research, we will vary the water discharge in order to modify the Froude number without affecting the non-dimensional depth.

3. Experimental observations

An experimental facility has been built at Politecnico di Milano in order to perform additional observations concerning the meandering flow pattern and to provide first quantitative data on the phenomenon.

This shallow reservoir has a length $L = 1.17$ m and a width $B = 0.78$ m. The width of the inlet channel is $b = 0.048$ m. This setup corresponds approximately to a 1:5 scale model of the reservoir used by Kantoush (2008). Experiments have been carried out in this scaled reservoir respecting the Froude similarity, leading to a discharge value $Q = 0.125$ l/s ($Re = 10,417$).

The aim is first to check whether a meandering flow pattern develops in the scaled reservoir for the same Froude numbers as in the larger reservoir. Detailed measurements of the velocity fields will be obtained in the near future to provide experimental data on the oscillation frequency of the meandering jet.

4. Numerical simulations by WOLF2D

The flow fields developing in the two experimental reservoirs (EPFL and Politecnico di Milano) have been simulated numerically with the model WOLF2D, developed by the University of Liege.

The model solves the divergence form of the shallow-water equations based on a finite volume scheme applied on multiblock structured grids. The advective fluxes are computed by a self-developed flux vector splitting method (Erpicum et al., 2010), while the turbulent fluxes are simply evaluated by means of a centred scheme (Erpicum et al., 2009). The time integration was performed here by means of a Runge-Kutta algorithm. A complete description of the computational model can be found in Dewals et al. (2008).

This model has already proven its validity and efficiency for the analysis of flows in shallow reservoirs (Dewals et al., 2008; Dufresne et al., 2011) as well as for numerous other applications including complex turbulent flows (Erpicum et al., 2009; Roger et al., 2009) and geophysical flows (Dewals et al. 2011; Ernst et al., 2010; Erpicum et al., 2010).

4.1 Reservoir 6 m × 4 m

For a reservoir geometry characterized by $L = 6$ m and $B = 4$ m, Kantoush (2008) showed that the flow pattern corresponds to a central meandering jet when the water depth is decreased from 0.2 m down to 0.15, 0.10 or 0.075 m, while keeping the inflow discharge constant ($Q = 7$ l/s) and thus also the Reynolds number. Here, the aim was to verify whether the numerical model is able to predict such a meandering flow pattern for the same geometric and hydraulic condition as in Kantoush's observations.

Table 1 confirms that the simulations succeed in predicting the meandering flow pattern for the same water depths as reported in Kantoush (2008). A typical example of an instantaneous velocity map produced by the numerical model is given in Figure 1.

h [m]	h/b	Froude Fr_{in} [-]	Experiments Kantoush ($Q=7$ l/s)	WOLF 2D Simulations	Period T [s]	Strouhal St [-]
0.2	0.8	0.1	Not meandering	Not meandering	-	-
0.15	0.6	0.15	Meandering	Meandering	7.3	0.18
0.1	0.4	0.28	Meandering	Meandering	7.8	0.11
0.075	0.3	0.43	Meandering	Meandering	7.4	0.09

Table 1–Tested configurations for the reservoir 6 m × 4 m, with four different water depths: 0.075 – 0.10 – 0.15 – 0.20 m.

As detailed in Table 1, besides the inlet Froude number of the experiment Fr_{in} , a Strouhal number St has also bee evaluated based on the inlet channel width b :

$$St = \frac{b \cdot f}{V_{in}}, \quad (1)$$

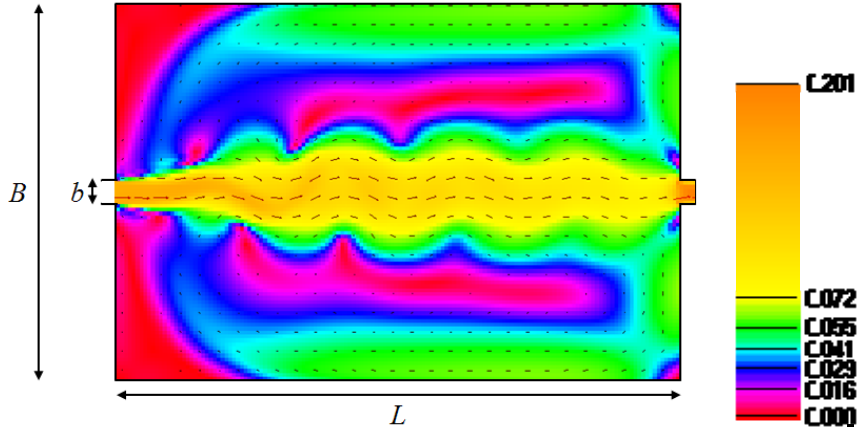


Figure 1- Velocity map of the meandering jet, simulated for the reservoir $6 \text{ m} \times 4 \text{ m}$ ($h = 0.075 \text{ m}$, $Q = 0.007 \text{ m}^3/\text{s}$). The color scale indicates the velocity magnitude [m/s].

where V_{in} is the velocity in the inlet channel: $V_{in} = Q / (bh)$, f is the oscillation frequency of the transversal velocity ($f = 1 / T$) and T is the oscillation period. The oscillation period of the transversal velocity has been verified to correspond to the oscillation period of the entire jet.

The meandering flow pattern develops when the Froude number is higher than 0.1, as shown both by the experimental and the numerical results (Table 1).

The oscillation period T keeps an approximately constant value close to 7.5 s and is not significantly affected by the varying non-dimensional depth (Table 1). Similarly, the oscillation period remains almost constant when the inlet Froude number varies by a factor three. It can thus be concluded that the Froude number and its corresponding geometrical parameter, the non-dimensional depth, have not a significant influence on the oscillation period of the jet.

In contrast, the Strouhal number is strongly affected by changes in the Froude number. Paragraph 7 focuses on the exact relationship between these two non-dimensional numbers.

4.2 Reservoir $1.17 \text{ m} \times 0.78 \text{ m}$

The numerical model has next been used to analyze the meandering flow patterns observed in the experimental setup of Politecnico of Milano ($L = 1.17 \text{ m}$, $B = 0.78 \text{ m}$, $b = 0.048 \text{ m}$). Four different water depths have been considered (0.04 – 0.03 – 0.02 – 0.015 m), leading to approximately the same inlet Froude number as for the configurations tested in the larger reservoir of EPFL. The discharge was set to $Q = 0.125 \text{ l/s}$ according to the Froude similarity law. Nonetheless, the inlet Froude numbers are not exactly the same due to slight discrepancies in the geometrical scaling of the reservoir inlet channel.

The objective is to verify whether the same meandering flow fields as found in the $6 \text{ m} \times 4 \text{ m}$ reservoir can be reproduced at a smaller scale, in order to evaluate the possible onset of scale effects.

Table 2 presents the oscillation periods of the transversal velocity obtained from the performed numerical simulations, as well as the corresponding Strouhal numbers.

The meandering flow pattern is observed to appear for the same hydraulic conditions as in the larger reservoir, whereas the oscillation period is found to be shorter. On the contrary, the Strouhal number remains virtually the same, as it was expected from the Froude similarity. Consequently, no significant scale affects have been detected and the meandering flow pattern may be studied equally well in both reservoirs.

Although ,the Froude and Strouhal number are almost equal in both reservoirs for the performed experiments, as well as the ratio h/b , the Reynolds number of the $1.17 \text{ m} \times 0.78 \text{ m}$ reservoir (10,400) is one order of magnitude lower than the Reynolds number of the $6 \text{ m} \times 4 \text{ m}$ reservoir (112,000). Nonetheless, the flow remains in turbulent regime in both cases.

h [m]	h/b	Froude Fr_{in} [-]	Experiments $Q = 0.125 \text{ l/s}$	WOLF 2D Simulations	Period T [s]	Strouhal St [-]
0.04	0.83	0.1	Not meandering	Not meandering	-	-
0.03	0.63	0.16	Meandering	Meandering	3.35	0.17
0.02	0.42	0.29	Meandering	Meandering	3.35	0.11
0.015	0.31	0.45	Meandering	Meandering	3.8	0.07

Table 2 – Tested configurations for the reservoir $1.17 \text{ m} \times 0.78 \text{ m}$,
with four different water depths: $0.015 - 0.02 - 0.03 - 0.04 \text{ m}$

5. Computation of the oscillation period

The oscillation periods presented in Tables 1 and have been evaluated according to the following two-step procedure:

- first, time series of the transversal velocity component in different points of the reservoir (five points along the central axis of the reservoir) were extracted from the simulation results (Figure 2);
- next, using a dedicated Matlab routine, the discrete Fourier transform $|Y(T)|$ of these temporal signals was computed in order to identify the dominant frequencies and thus the oscillation period (Figure 3).

The computed oscillation frequency of transversal velocity was the same for all the points sampled along the reservoir axis, confirming that the oscillation period of the meandering jet may be deduced from the oscillation period of the transversal velocity component.

Moreover, videos of the time evolution of the velocity field in the whole reservoir have been produced from the 2D unsteady simulation results, in order to confirm visually that the oscillation of the jet observed on the video corresponds to the value computed by the discrete Fourier transform. The oscillation periods of about 7.5 s for the $6 \text{ m} \times 4 \text{ m}$ reservoir and of about 3.5 s for the $1.17 \text{ m} \times 0.78 \text{ m}$ reservoir could be confirmed.

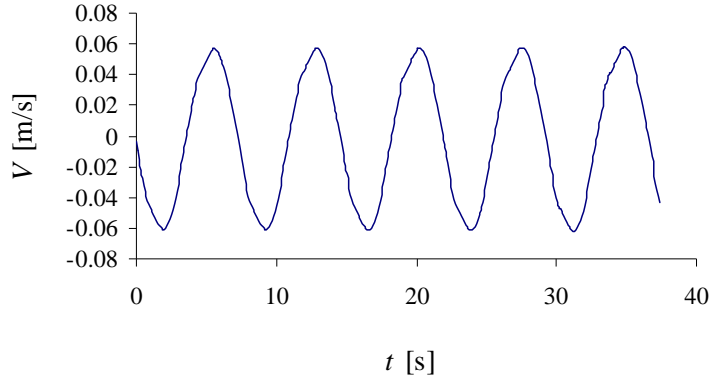


Figure 2– Temporal signal of the transversal velocity v in one point along the axis of the meandering jet (reservoir $6\text{ m} \times 4\text{ m}$)

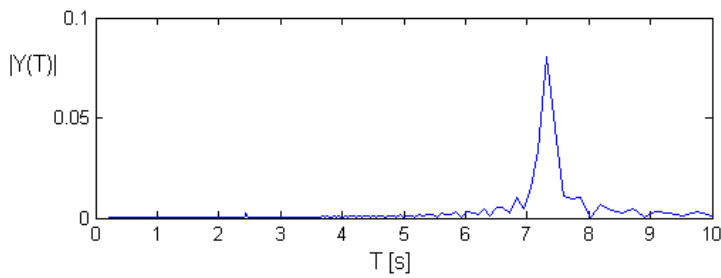


Figure 3 – Spectrum of the transversal velocity v in one point along the axis of the meandering jet (reservoir $6\text{ m} \times 4\text{ m}$)

6. Sensitivity analysis

In parallel with the simulations presented in the previous paragraphs, a sensitivity analysis has been carried out with respect to the grid resolution and to other numerical parameters of the simulations. The objective was to confirm that the simulated periodic flow patterns are not caused by numerical effects, but that they do represent the physical oscillations as could be qualitatively observed in the experimental tests.

In particular, we have analyzed the influence on the oscillation frequency of the following parameters:

- Courant number (tested values: $0.5 - 0.25 - 0.125$);
- sampling frequency (tested values: $0.5-0.1-0.05$ s);
- time discretization algorithm (3-step Runge Kutta method of first order accuracy: RK31 vs. 2-step Runge Kutta method of second order accuracy: RK22);
- grid resolution (Calculus of the Global Convergence Index GCI).

6.1 Courant number

By performing simulations with different Courant numbers, it was observed that this parameter has no significant influence on the simulation results. Therefore, the Courant number can be increased up to the maximum value compatible with the stability of the simulation, namely the Courant Friedrich Levy condition.

6.2 Sampling frequency

Figure 4 compares time series of the velocity obtained using two different sampling frequencies: 2 Hz (blue line) and 10 Hz (red line). Both signals are found to enable a satisfactory representation of the velocity oscillations. Nonetheless, a sampling frequency of 10 Hz was been generally adopted for post-processing the simulation results, since it provides a higher accuracy without increase in the computational cost. Obviously, the sampling frequency also influences the maximum frequency which can be detected. This maximum frequency equals half of the sampling frequency: 5 Hz.

6.3 Time discretization

As can also be seen in Figure 4, the two tested Runge Kutta algorithms lead to practically the same oscillation frequency. A limited influence can only be observed in the amplitude of the velocity oscillations: the first order accurate Runge Kutta algorithm (RK31) tends to smooth the peaks of the signal, slightly damping the amplitude of velocity oscillations. In contrast, the second order accurate Runge Kutta algorithm (RK22) reproduces more accurately the peaks. As a result, the second order accurate Runge-Kutta method has been adopted for all simulations, due to its higher accuracy for representing unsteady flows.

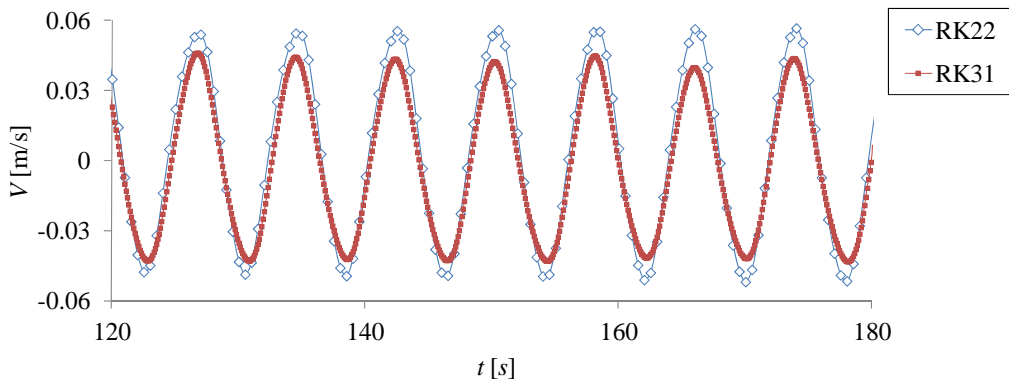


Figure 4— Influence of the time discretization algorithm on the oscillation frequency. Temporal signal of velocity (RK 22 with a sampling frequency of 2 Hz vs. RK31 with a sampling frequency of 10 Hz).

6.4 Grid resolution

In order to confirm the grid independency of the results, the influence of the grid resolution on the computed oscillation frequency has been checked. For this purpose, a Grid Convergence Index (GCI) was calculated according to the procedure suggested by Roache (1994; 1997). The value of this GCI provides an error band between the numerical result for the considered grid solution and the exact solution f_{exact} of the continuous equations.

The GCI has been calculated based on the results of simulations conducted on two different grids: a coarser one ($h_2 = 0.008$ mm) and a finer one ($h_1 = 0.004$ mm). The results of this analysis are presented in Table 3.

Since the resulting error on the oscillation frequency was found to be particularly low (0.65%), the coarser grid has been selected to perform all subsequent simulations due to the very significant gain in computational time it provides compared to the finer grid.

Cell size [mm]	Period T [s]	GCI	Estimate of f_{exact}
8	3.85	0.65%	3.83÷3.88
4	3.86	0.16%	3.85÷3.87

Table 3 – Period of oscillation and GCI for the reservoir characterized by $L = 1.17$ m and $B = 0.78$ m.

7. Strouhal-Froude relationship

A relationship has been established between the inlet Froude number and the Strouhal number characterizing the oscillation frequency of the meandering jet.

As can be seen in Figure 5, a logarithmic regression has been found to describe satisfactorily the link between the Froude and Strouhal numbers ($R^2 = 0.97$):

$$St = 0.09 \cdot \ln(Fr_{in}) + 0.002 \quad (2)$$

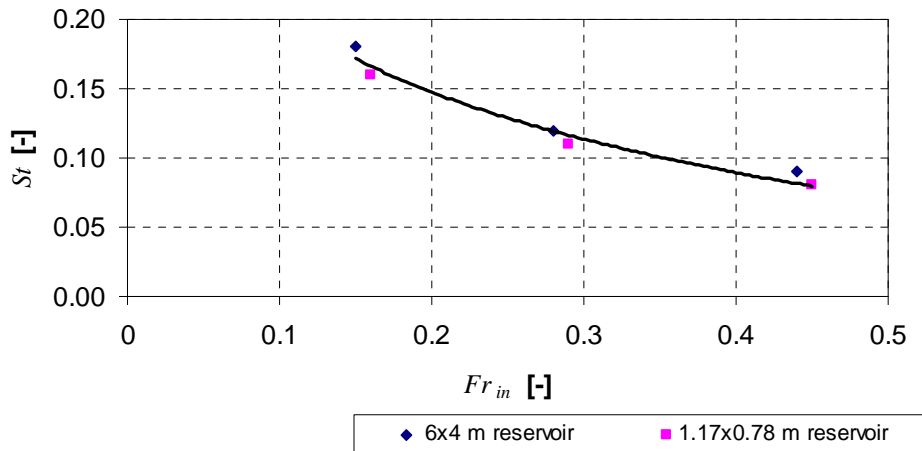


Figure 5– Strouhal-Froude relationship for the meandering jet

So far, the evaluation of these non-dimensional numbers is entirely based on the simulations performed for the $6\text{ m} \times 4\text{ m}$ and $1.17\text{ m} \times 0.78\text{ m}$ reservoirs. A more robust confirmation of relation (2) will be obtained by expanding the presently available data with more numerical and experimental results.

8. Conclusions and perspectives

The study presented here provides a first insight into some aspects of the development of a central meandering flow in shallow rectangular reservoirs. In one geometric configuration of the reservoir, the oscillation frequency of the jet has been studied for different Froude numbers and at two different scales. Numerical simulations have confirmed that the meandering flow pattern arises for inlet Froude numbers satisfying $Fr_{in} > 0.1$ (i.e. $h/b < 0.8$). It has also been shown that a variation of the Froude number in a broad range (0.15-0.44) does not influence the value of the oscillation period. In contrast, a logarithmic relationship between the Froude and the Strouhal numbers has been found.

The subsequent steps of this work will include the following:

- investigate the possible formation of the meandering jet for other geometrical reservoir configurations, characterized by different aspect ratio L/B and expansion ratio B/b ;
- identify secondary frequencies present in the velocity time series;
- study other characteristics of the meandering flow pattern, such as the spatial amplitude of the meandering jet as a function of the geometry of the reservoir;
- collect experimental data of velocity in the facility of Politecnico di Milano, in order to obtain confirmations of the oscillation frequency simulated by WOLF2D.

References

- Camnasio, E., Orsi, E., Schleiss, A.J. (2011). Experimental study of velocity fields in rectangular shallow reservoirs. *J. Hydr. Res.* Vol. 49:3, 352-358.
- Chen, D, Jirka GH. (1995). Experimental study of plane turbulent wakes in a shallow water layer. *Fluid Dynamics Research.* 16(1):11-41.
- Davidson, M.R., Lawson, N.J. (1999). Numerical prediction of submerged oscillating jet flow. Second International Conference on CFD in the Minerals and Processes Industries, CSIRO, Melbourne, Australia, 6-8 December 1999.
- Dewals, B.J., Kantoush, S.A., Erpicum, S., Pirotton, M., Schleiss, A.J. (2008). Experimental and numerical analysis of flow instabilities in rectangular shallow basins. *Env. Fluid Mech.* 8(1), 31-54.
- Dewals, B. J., Erpicum, S., Detrembleur, S., Archambeau, P. and Pirotton, M. (2011). Failure of dams arranged in series or in complex, *Nat. Hazards.* 56(3), 917-939.
- Dufresne, M., Dewals, B.J., Erpicum, S., Archambeau, P., Pirotton, M. (2010). Classification of flow patterns in rectangular shallow reservoirs. *J. Hydraulic Res.* 48(2), 197-204.
- Dufresne, M., Dewals, B. J., Erpicum, S., Archambeau, P., and Pirotton, M. (2011). Numerical investigation of flow patterns in rectangular shallow reservoirs. *Engineering applications of computational fluid dynamics,* 5(2), 247-258.
- Ernst, J., Dewals, B. J., Detrembleur, S., Archambeau, P., Erpicum, S. and Pirotton, M. (2010). Micro-scale flood risk analysis based on detailed 2D hydraulic modelling and high resolution land use data. *Nat. Hazards,* 55(2), 181-209.
- Erpicum, S., Meile, T., Dewals, B. J., Pirotton, M., Schleiss, A. J. (2009). 2D numerical flow modelling in a macro-rough channel. *Int. J. Numer. Methods Fluids,* 61(11), 1227-1246.
- Erpicum, S., Dewals, B.J., Archambeau, P. and Pirotton, M. (2010). Dam-break flow computation based on an efficient flux-vector splitting. *Journal of Computational and Applied Mathematics,* 234(7), 2143-2151.
- Honeylands, T.A., Molloy N.A. (1995). Oscillations of submerged jets confined in a narrow deep rectangular cavity. Twelfth Australian Fluid Mechanics Conference. University of Sydney, Australia, pp. 493 – 496.
- Kantoush, S.A. (2008). Experimental study on the influence of the geometry of shallow reservoirs on flow patterns and sedimentation by suspended sediments, PhD thesis 4048. EPFL, Lausanne.
- Roache, PJ. (1997). Quantification of uncertainty in Computational Fluid Dynamics. *Annual Review of Fluid Mechanics.* 29:123-160.
- Roache, PJ. (1994). Perspective: a method for uniform reporting of grid refinement studies. *Journal of Fluids Engineering.* 116:405–413.